Journal of Hazardous Materials 193 (2011) 10–16

Contents lists available at ScienceDirect

Journal of Hazardous Materials

journal homepage: www.elsevier.com/locate/jhazmat

Synthesis of magnetic wheat straw for arsenic adsorption

Ye Tian[a,b,c], Min Wu[a,*], Xiaobo Lin[b,c], Pei Huang[b,c], Yong Huang[a,b,d,**]

[a] State Engineering Research Center of Engineering Plastics, Technical Institute of Physics and Chemistry, Chinese Academy of Sciences, Beijing 100190, China
[b] State Key Laboratory of Polymer Physics and Chemistry, Beijing National Laboratory for Molecular Sciences, Institute of Chemistry, Chinese Academy of Sciences, Beijing 100190, China
[c] Graduate School, Chinese Academy of Sciences, Beijing 100039, China
[d] Laboratory of Cellulose and Lignocellulosics Chemistry, Guangzhou Institute of Chemistry, Chinese Academy of Sciences, Guangzhou 510650, China

ARTICLE INFO

Article history:
Received 14 December 2010
Received in revised form 23 March 2011
Accepted 23 April 2011
Available online 6 May 2011

Keywords:
Magnetic wheat straw
Arsenic
Adsorption

ABSTRACT

Magnetic wheat straw (MWS) with different Fe_3O_4 content was synthesized by using in-situ co-precipitation method. It was characterized by powder X-ray diffraction (XRD) and vibrating sample magnetometer (VSM). This material can be used for arsenic adsorption from water, and can be easily separated by applied magnetic field. The introduction of wheat straw template highly enhanced the arsenic adsorption of Fe_3O_4. Among three adsorption isotherm models examined, the data fitted Langmuir model better. Fe_3O_4 content and initial pH value influenced its adsorption behavior. Higher Fe_3O_4 content corresponded to a higher adsorption capacity. In the pH range of 3–11, As(V) adsorption was decreased with increasing of pH; As(III) adsorption had the highest capacity at pH 7–9. Moreover, by using 0.1 mol L^{-1} NaOH aqueous solution, it could be regenerated. This work provided an efficient way for making use of agricultural waste.

1. Introduction

Arsenic pollution has become a major environment concern these years. It is originated from both natural activities (like oxidative weathering and geochemical reactions) [1] and the anthropogenic activities. Arsenic mainly exists in the inorganic anion forms of AsO_2^-(III) and AsO_4^{3-}(V). Intake of arsenic leads to cancers in skin, lungs, liver, kidney and bladder, and can also cause hypertension, cardiovascular disease and skin disease [2]. For its high toxicity, the World Health Organization has specified the arsenic concentration in drinking water should be no more than 0.01 mg L^{-1} [3].

Adsorption is an effective technique for treating arsenic-contaminated water. Many materials can be used as adsorbents, such as activated carbon [4], chitosan [2], alumina [5], granular ferric hydroxide [1], goethite [6], activated sludge [7] and lanthanum-impregnated silica gel [8]. However, for a normal adsorbent, the adsorbent–arsenic complex needs to be separated and collected from water after adsorption, through filtration or precipitation. Magnetic adsorbent shows predominance over these adsorbents due to its ease in separation [9,10]. After treatment, it can be collected using low-field magnets easily, producing no contaminants such as flocculants. There have been some magnetic adsorbents reported, such as magnetic cellulose beads for organic dye adsorption [11], magnetic alginate for copper [9], organic arsenic [12] and organic dye adsorption [13], magnetic multiwall carbon nanotube for europium adsorption [14], magnetic chitosan beads for chromium adsorption [15] and a magnetic chelating resin for heavy metal ion adsorption [16]. Our aim is to find a novel, cost-effective magnetic adsorbent for inorganic arsenic.

As an agricultural waste, wheat straw has a high yield every year. Only in China, its annual production is estimated to be at least 600 million tons. In addition, it has a production of 170 million ton per year in European countries [17]. However, most of the wheat straw has been burnt for cooking or heating, or been left directly to decompose. These treatments will not only waste natural resources, but also cause environmental pollutions. Therefore, it is necessary to make the best use of wheat straw. Our group has made a comprehensive study for the component, structure and morphology of wheat straw [18,19]. Wheat straw has a vascular bundle structure, which will provide additional surface for chemical modification. It also has complicated components including lignin, hemicellulose, cellulose, pectin, protein and fatty acid. The wheat straw is abundant in hydroxyl groups. The hydroxyl groups can provide chemical reaction sites and adsorb iron ions to grow Fe_3O_4 crystal. In this study, we use the agricultural waste wheat straw as template, grow Fe_3O_4 nano- or micro-particles on

* Corresponding author at: State Engineering Research Center of Engineering Plastics, Technical Institute of Physics and Chemistry, Chinese Academy of Sciences, Beijing 100190, China.
** Corresponding author.
E-mail address: wumin@mail.ipc.ac.cn (M. Wu).

0304-3894/$ – see front matter © 2011 Elsevier B.V. All rights reserved.
doi:10.1016/j.jhazmat.2011.04.093

its surface, and then investigate its potential application in arsenic adsorption.

2. Experimental

2.1. Materials

Mature wheat straw was collected from the countryside and mechanically grinded into fragments, with a BET surface area in a dry state of 4.73 $m^2\ g^{-1}$. Iron(II) sulfate heptahydrate ($FeSO_4{\cdot}7H_2O$), iron (III) chloride hexahydrate ($FeCl_3{\cdot}6H_2O$) (both from Sinopharm Chemical Reagent Co., Ltd) and ammonia solution ($NH_3{\cdot}H_2O$, 25%, Beijing Chemicals Co.) were used for Fe_3O_4 synthesis. Sodium arsenite ($NaAsO_2$) and sodium arsenite dibasic ($Na_2HAsO_4{\cdot}7H_2O$) (both from Beijing Chemicals Co.) were used to obtain the solutions of AsO_2^- and AsO_4^{3-}. All the agents were analytical grade and were used without further purification.

2.2. Synthesis of Fe_3O_4/wheat straw

The Fe_3O_4/wheat straw composites were synthesized by in-situ co-precipitation, which is a classical method for Fe_3O_4 generation. The chemical reaction of Fe_3O_4 formation can be written as Eq. (1):

$$Fe^{2+} + 2Fe^{3+} + 8OH^- \rightarrow Fe_3O_4 + 4H_2O \quad (1)$$

In this study, about 0.5 g ground wheat straw fragments were suspended in a 50 mL mixed solution of $FeSO_4$ and $FeCl_3$ (molar ratio of Fe^{3+} to Fe^{2+} is 2/1) under N_2. After a certain amount of $NH_3{\cdot}H_2O$ (25%) was added into the system, the temperature was raised to 70 °C and held at that for 4 h. The fabricated wheat straw was washed several times by deionized water and separated by a magnet, and then dried in vacuum. The un-reacted wheat straw was coded as WS. The synthesized magnetic wheat straw samples were coded as MWS1, MWS2 and MWS5, the total iron ion concentrations in the reaction system of which were 0.1 mol L^{-1}, 0.2 mol L^{-1} and 0.5 mol L^{-1}, respectively. The corresponding amount of $NH_3{\cdot}H_2O$ (25%) added was 2 mL, 4 mL and 10 mL, respectively. We also synthesized the bare magnetite for comparison. The synthesizing process and formula were the same as MWSs, except that there is no wheat straw in the reaction. The obtained samples with total iron concentrations of 0.1 mol L^{-1}, 0.2 mol L^{-1} and 0.5 mol L^{-1} were coded as M1, M2 and M5, respectively.

2.3. Adsorption and desorption of arsenic

In this study, the solutions of As(III) and As(V) were obtained respectively by dissolving sodium arsenite ($NaAsO_2$) and sodium arsenite dibasic ($Na_2HAsO_4{\cdot}7H_2O$) into deionized water. The effects of Fe_3O_4 content, initial arsenic concentration, initial pH value and adsorbent dose on the equilibrium adsorption capacity were investigated. The adsorption isotherms were also studied, with the initial ion concentration between 1 mg L^{-1} and 28 mg L^{-1}, at the original pH value of the solution (without adding acid or alkali). For the adsorption capacity tests, magnetic wheat straw was suspended in aqueous arsenic solutions with a known concentration and shaken with a speed of 250 rpm at 30 °C for 12 h. The adsorption capacity q (mg g^{-1}) was calculated from the following expression (Eq. (2)):

$$q = \frac{(C_0 - C_e)V}{m} \quad (2)$$

where C_0 and C_e represent the initial and equilibrium concentrations of the anion solutions, respectively. V and m are the solution volume and adsorbent mass, respectively. The adsorbent dose (m/V) was kept 0.5 g L^{-1} for all the experiments except the adsorbent dose study.

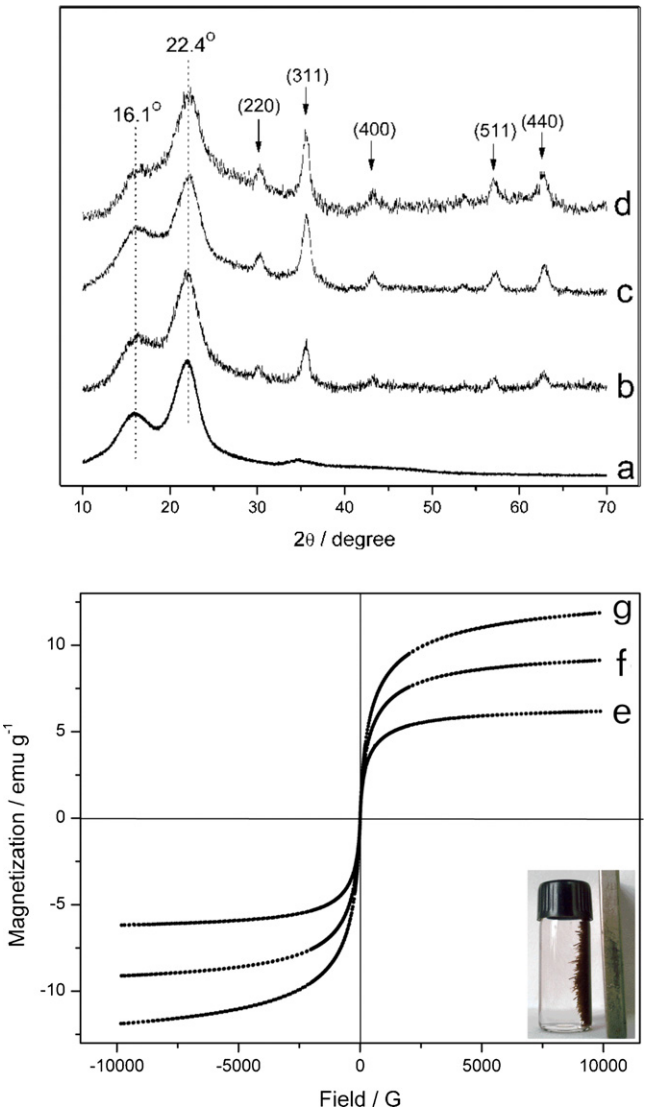

Fig. 1. The powder X-ray diffraction patterns of (a) WS, (b) MWS1, (c) MWS2 and (d) MWS5. The magnetic hysteresis loops of (e) MWS1, (f) MWS2 and (g) MWS5 at 298 K. *Inset*: The photograph of MWS5 with an external magnetic field.

The desorption of arsenic can be achieved by using dilute HCl [20] or NaOH aqueous solution [21]. In our study, we used 0.1 mol L^{-1} NaOH solution for desorption, considering the Fe_3O_4 particles will be dissolved when pH < 2. The adsorbent carrying arsenic was shaken in the desorption solution at a speed of 250 rpm at 30 °C for 3 h. Then the adsorbent was washed with deionized water. After being freeze-dried, the regenerated adsorbent can be used for arsenic adsorption again to measure its recycling efficiency.

2.4. Characterization of magnetic wheat straw

The specific surface area of wheat straw in a dry state was measured by a Micromeritics ASAP 2020 M Nitrogen System. Powder X-ray diffraction (XRD) was carried out on a D8 Focus (Bruker) XRD diffractometer for the crystalline characterization. The magnetic properties of the magnetic wheat straw were investigated using a vibrating sample magnetometer (VSM, Lake Shore 7307) at room temperature in the applied magnetic field from −10,000 G to 10,000 G. The concentrations of arsenic were measured using Thermo ICAP6000 Inductively Coupled Plasma.

Table 1
The arsenic adsorption capacity of wheat straw loaded Fe_3O_4 and bare Fe_3O_4. The equilibrium adsorption capacity (q_e) was measured in As(V) solution of 10 mg L^{-1}.

	q_e (mg As g^{-1} Fe_3O_4)
Wheat straw loaded Fe_3O_4	
MWS1	30.24
MWS2	27.24
MWS5	24.14
Bare Fe_3O_4	
M1	6.98
M2	6.31
M5	6.02

3. Results and discussions

3.1. Structure and magnetic properties

The powder XRD patterns of WS and MWSs are shown in Fig. 1a–d. Wheat straw consists of mainly crystalline cellulose, and noncrystalline hemicellulose and lignin [18]. All the graphs have the diffraction peaks at $2\theta = 16.1^\circ$ and 22.4° for cellulose I crystalline form, which is assigned to most natural cellulose [18]. For MWS1, MWS2 and MWS5, the peaks at $2\theta = 30.3^\circ, 35.6^\circ, 43.3^\circ, 57.4^\circ$ and 62.8° are the characteristic peaks of Fe_3O_4 and are assigned to the (2 2 0), (3 1 1), (4 0 0), (5 1 1) and (4 4 0) planes of Fe_3O_4, respectively. The Fe_3O_4 crystal has been successfully grown onto the wheat straw template. As can be seen, when the total iron ion concentrations in the reaction increase, the relative intensities of Fe_3O_4 peaks become stronger, indicating an increase of Fe_3O_4 loading in the wheat straw matrix.

The magnetic hysteresis loops at 298 K of the MWSs are shown in Fig. 1e–g. All of them show typically superparamagnetic behavior, which means the magnetic material can response to an applied magnetic field without any permanent magnetization, with the loop area being zero. The saturated magnetizations for MWS1, MWS2 and MWS5 are 6.18, 9.12 and 11.87 emu g^{-1}, depending on the Fe_3O_4 content. Materials with superparamagnetic behavior can be easily separated from the solution with the help of an external magnetic field (see Fig. 1, inset). Based on this feature, the MWSs will be very advantageous to be used as materials for adsorption and separation.

3.2. Adsorption properties

3.2.1. Effect of Fe_3O_4 content and adsorption isotherms

Fig. 2a shows the adsorption behaviors of MWSs for As(III) and As(V) at different initial ion concentrations, with the adsorbent dose being 0.5 g L^{-1}. In Fig. 2a, the equilibrium adsorption capacity (q_e) increases with the initial arsenic concentration (C_0). And the adsorption capacity for As(V) is higher than As(III), which is due to the more mobility of As(III) [22]. Comparing the MWSs with different Fe_3O_4 content, the adsorption capacity is in the order of MWS5 > MWS2 > MWS1. That means Fe_3O_4 is an effective component of arsenic adsorption. We compared the adsorption capacity of MWSs with pure wheat straw and the synthesized bare magnetite. The wheat straw itself does not have the capacity to adsorb arsenic. Its main function is to provide a template with high specific area for Fe_3O_4 loading. By comparing the arsenic adsorption capacity of Fe_3O_4 with and without the template in Table 1, we can see the adsorption capacities of Fe_3O_4 loading onto the wheat straw are much higher than the bare ones. Hereby the introduction of wheat straw template can effectively enhance the adsorption capacity. The reason may be that the template can prevent Fe_3O_4 particles from aggregating in adsorption process, and increase the effective adsorption area, resulting in the highly enhancement of adsorption capacity.

Table 2
Langmuir, Freundlich and Temkin parameters for adsorption isotherms at 30 °C. The r^2 values correspond to the linear correlation coefficients.

	Langmuir parameters		
	Q_0 (mg g^{-1})	b (L mg^{-1})	r^2
As(III)			
MWS1	0.760	0.669	0.921
MWS2	2.313	0.266	0.935
MWS5	3.898	0.270	0.899
As(V)			
MWS1	4.018	0.133	0.952
MWS2	6.683	0.186	0.982
MWS5	8.062	0.216	0.977
	Freundlich parameters		
	K_f (mg g^{-1})	n	r^2
As(III)			
MWS1	0.533	10.02	0.573
MWS2	0.980	4.804	0.805
MWS5	1.560	4.328	0.892
As(V)			
MWS1	0.561	1.771	0.969
MWS2	1.168	1.908	0.976
MWS5	1.645	2.086	0.989
	Temkin parameters		
	A_T (L mg^{-1})	b_T (kJ mol^{-1})	r^2
As(III)			
MWS1	3476.4	38.888	0.508
MWS2	25.879	8.528	0.723
MWS5	22.893	4.945	0.752
As(V)			
MWS1	1.806	3.152	0.940
MWS2	2.485	1.890	0.955
MWS5	3.267	1.639	0.949

In order to examine the adsorption mechanism and surface properties of the MWSs, the adsorption isotherms are investigated and fitted by Langmuir model, Freundlich model and Temkin model. The Langmuir model [23] assumes monolayer adsorption with uniform energies of adsorption on the surface. The Freundlich model [24] is based on a multilayer adsorption with the adsorption energy decreases with the surface coverage. Temkin isotherm [25] assumes that the fall in the heat of adsorption is linear rather than logarithmic, as implied in the Freundlich equation. The three models can be expressed as Eqs. (3)–(5), respectively:

$$\frac{C_e}{q_e} = \frac{1}{bQ_0} + \frac{C_e}{Q_0} \tag{3}$$

$$\ln q_e = \ln\ K_f + \frac{1}{n} \ln C_e \tag{4}$$

$$q_e = \frac{RT}{b_T} \ln A_T + \frac{RT}{b_T} \ln C_e \tag{5}$$

where C_e (mg L^{-1}) and q_e (mg g^{-1}) are the concentration and adsorption capacity at equilibrium, respectively. Q_0 (mg g^{-1}) and b (L mg^{-1}) are Langmuir constants. K_f (mg g^{-1}) and n are Freundlich constants measuring the adsorption capacity and the adsorption intensity, relatively. A_T (L mg^{-1}) and b_T (J mol^{-1}) are the Temkin constants. R is the universal gas constant 8.314 J mol^{-1} K^{-1} and T is the absolute temperature 303 K. The linear plots fitting by the three models for MWSs adsorbing As(III) and As(V) are drawn in Fig. 2b–d and the parameters can be evaluated from the linear plots (shown in Table 2). Based on Table 2, the linear correlation coefficients r^2 is in the order of r^2 (Langmuir) > r^2 (Freundlich) > r^2 (Temkin). It indicates that the adsorption isotherms of As(III) and As(V) onto the MWSs fit Langmuir model better than Freundlich and Temkin models, and assumes that it is a monolayer adsorption process.

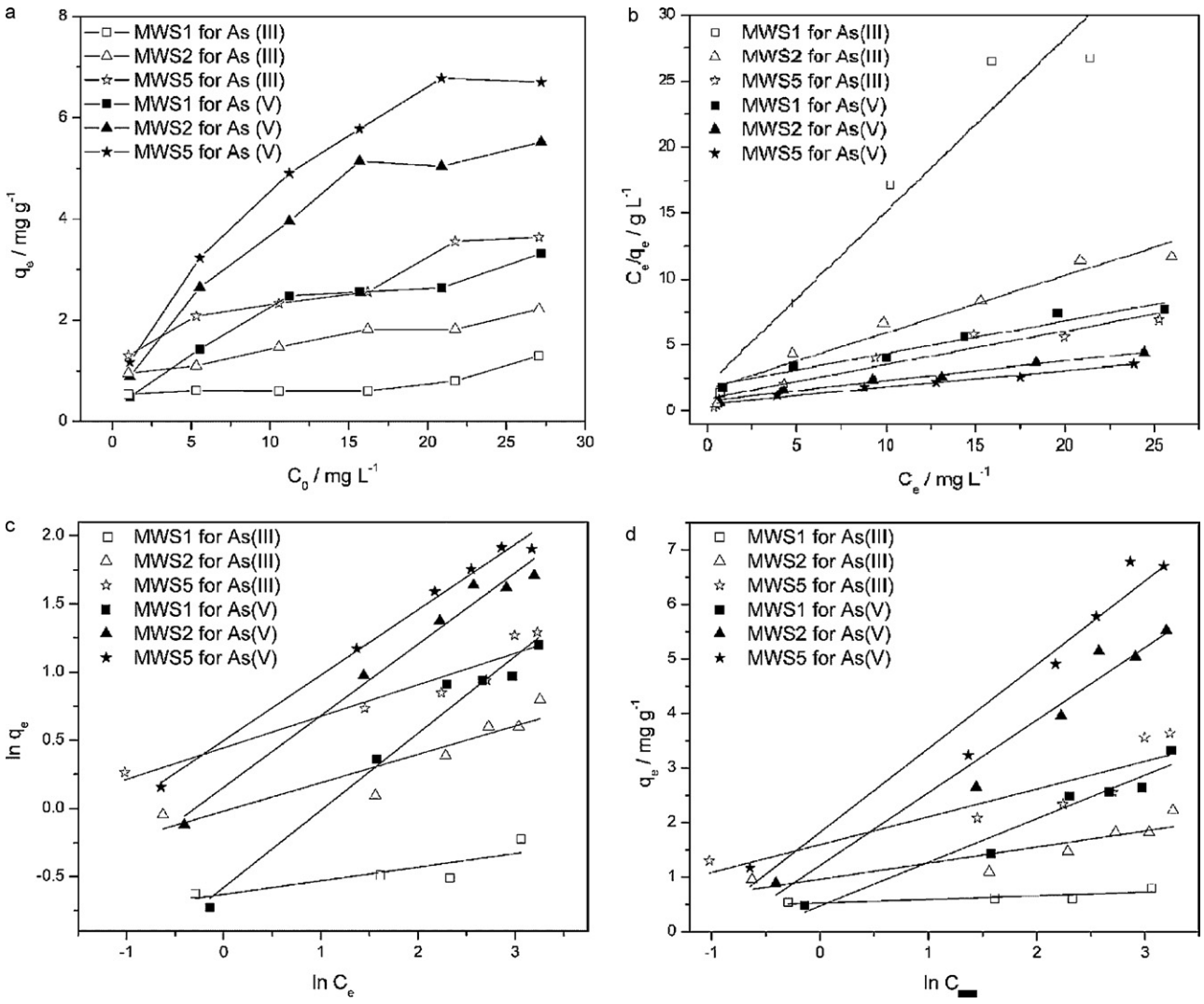

Fig. 2. (a) Effect of initial ion concentration and Fe_3O_4 content on the adsorption behavior for arsenic. Linear plots of adsorption isotherms at 30 °C fitting by (b) Langmuir, (c) Freundlich and (d) Temkin models.

In Langmuir model, the constant Q_0 measures the maximum adsorption capacity. From the values of Q_0 in Table 2, we can see that the maximum adsorption capacity for arsenic is in the order of MWS5 > MWS2 > MWS1, and the adsorption capacity for As(V) is higher than As(III). This rule is different from Amy Kan's and Kwang Kim's results [26,27], but agrees with Zhang's [28]. Comparing its Q_0 values with the other iron-based nonmagnetic adsorbents [29–31] and natural adsorbents [32] in Table 3, we can see that except an advantage of easy separation by external magnetic field, the adsorption capacity of MWSs is highly competitive to the nonmagnetic adsorbents. Among the magnetic adsorbents in Table 3 [26,33], the arsenic adsorption on Fe_3O_4 of our composite adsorbent is effective, but lower than the nano material. If we can control the Fe_3O_4 to be nano-particles, the arsenic adsorption capacity may be highly enhanced. That is our ongoing research work. In Langmuir model, the constant b is related to the separation factor or equilibrium parameter, R_L, which is defined as [34]:

$$R_L = \frac{1}{1 + bC_0} \quad (6)$$

where C_0 (mg L^{-1}) is the initial concentration of arsenic. In the C_0 range of our investigation, the value of R_L is 0.052–0.790 for As(III) and 0.146–0.883 for As(V). The R_L value lies between 0 and

Table 3
Comparison of the Langmuir capacity of different adsorbents for arsenic adsorption.

	Q_0 (mg g^{-1})		Reference
	As(III)	As(V)	
Iron hydroxide-coated alumina	7.65	15.9	[29]
Iron oxide-coated sand	0.029	–	[30]
Acidithiobacillus ferrooxidans BY-3	0.293	0.333	[31]
Natural laterite	0.17	–	[32]
Nano-$MnFe_2O_4$	93.8	90.4	[33]
Magnetite-reduced graphene oxide	10.20	5.27	[26]
MWS5	3.898 mg As g^{-1} MWS519.2 mg As g^{-1} Fe_3O_4	8.062 mg As g^{-1} MWS539.7 mg As g^{-1} Fe_3O_4	This study

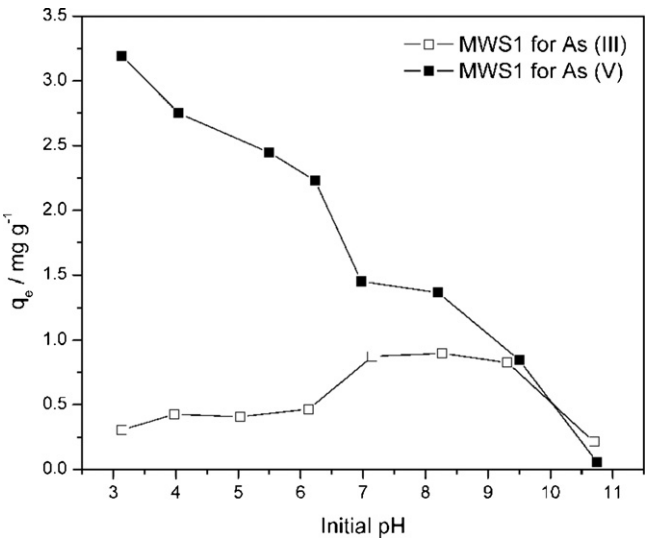

Fig. 3. Effect of initial pH value on the adsorption capacity of MWS1 for arsenic.

1, indicating that the arsenic adsorption on MWSs is a favorable process.

3.2.2. Effect of initial pH value

The arsenic adsorption behavior of magnetite materials is pH-dependent [10,35]. The surface hydroxyl groups on iron oxide can be protonated and de-protonated [12,35] and its intrinsic surface complexation constants have been used in previous studies [36]. The arsenic chemistry in water is also highly dependent on pH. At different pH, both arsenate and arsenite can be protonated into different species [37], and the specie types can be determined by their protonation constants [35]. The effect of initial pH value on the adsorption capacity in our study is shown in Fig. 3. The As(V) adsorption capacity decreased with pH, and the As(III) adsorption capacity has a highest value at pH 7–9. This phenomenon can be explained by surface complexation model, which has been used by Marmie, Janet and Hering et al. [35,36]. We can also explain it easily by the surface and arsenic charge. When pH is lower, the magnetite, which behaves as weak acid, can be protonated to form positive surface, which is beneficial to adsorb the anionic arsenic [12,38]. Therefore, the adsorption capacity is supposed to increase when pH value decreases, like the behavior of As(V) in Fig. 3. But for As(III), it dose not follow this rule. This phenomenon is attributed to the pH-dependence of As(III) [37]. For As(III), at pH < 9.2, the uncharged species $H_3AsO_3{}^0$ will predominate in water. This state of As(III) could not be adsorbed on the adsorbent surface for the missing of electrostatic attraction. So at lower pH, the q_e for As(III) will also decrease with the decreasing pH, leaving the highest q_e at pH 7–9.

3.2.3. Effect of adsorbent dose

Fig. 4a shows the effect of adsorbent dose on adsorption capacity and removal efficiency. The chosen adsorbent is MWS1, and the arsenic solution is 10 mg L^{-1} of As(V). The arsenic removal efficiency increased with the MWS1 dose. That is induced by the larger adsorption area and the increased number of active adsorption sites. Meanwhile, the effective surface area for adsorption actually decreased, caused by the partial aggregation of MWSs. This led to the reduction of adsorption capacity with MWS1 dose.

The adsorbent dose will also affect the distribution coefficient K_D, which describes the binding ability of adsorbent surface to an

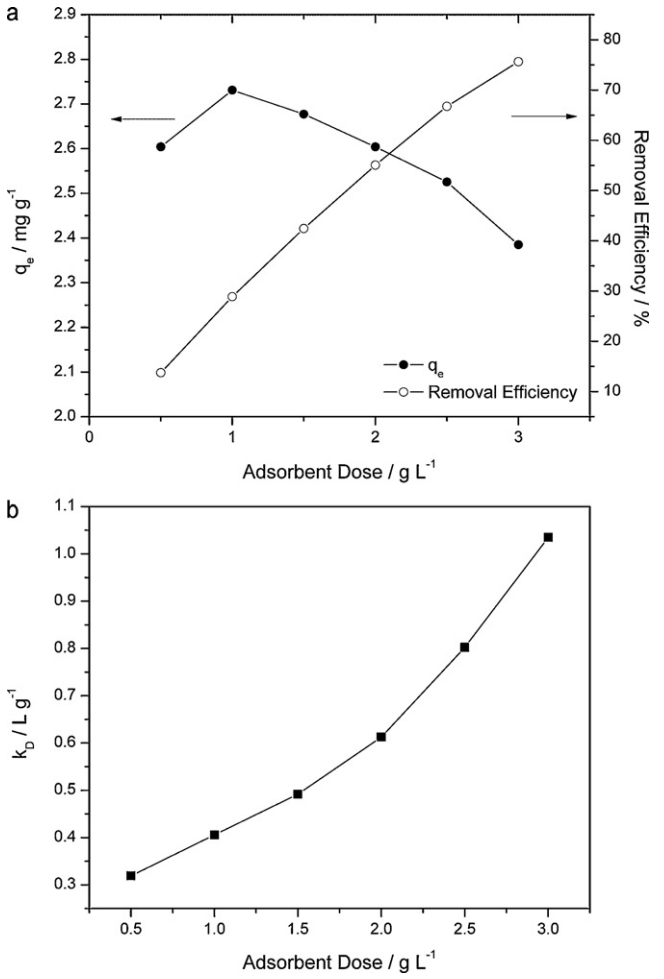

Fig. 4. The effect of adsorbent dose on (a) adsorption capacity, removal efficiency, and (b) distribution coefficient for As(V).

element, and can be calculated from the following expression (Eq. (7)):

$$K_D = \frac{C_S}{C_W} \quad (7)$$

where C_s and C_w are the element concentrations in solid adsorbents (mg g^{-1}) and in water (mg L^{-1}), respectively. At a given pH, the value of K_D for a settled element shows two different situations: (I) The K_D value stays the same with adsorbent dose. This implies that adsorbent surface is homogeneous. Our group has synthesized cellulose – g-PDMAEMA for arsenic and fluoride removal, and its surface obeys this rule [39]. (II) The K_D value will increase with the adsorbent dose. This situation means the adsorbent surface is heterogeneous. In Fig. 4b, MWS5 has a K_D increasing with the adsorbent dose, which implies that the surface of MWSs is heterogeneous. The detailed structure of the adsorption surface has been studied by Sherman group through XANES and EXAFS data. In their theory, the adsorption is based on the inner-sphere complexation of As on {1 0 0} surfaces of magnetite [40].

3.3. Desorption and regeneration

For practical use of an adsorbent, the regeneration of the material is very important to cut the cost. For this adsorbent, it can be regenerated by de-adsorbing arsenic using 0.1 mol L^{-1} NaOH aqueous solution. Fig. 5 shows the reusability of MWS5 for As(V) removal with the initial concentration being 10 mg L^{-1}. As evi-

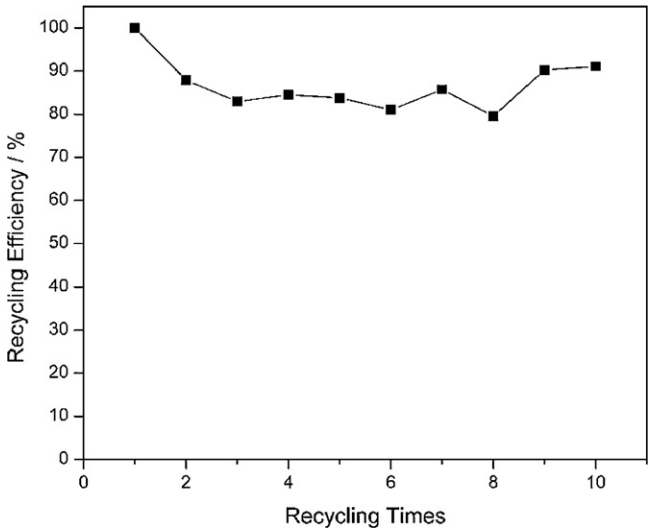

Fig. 5. The recycling efficiency of MWS5 for As(V) with the initial concentration being 10 mg L^{-1}.

dent, in the 10-time-usage of the adsorbent, the recycling efficiency keeps above 80%. So this material can be used for arsenic removal efficiently for at least 10 times. It will be very advantageous in real applications.

4. Conclusions

In this study, we synthesized magnetic bio-adsorbent for arsenic by using agricultural waste wheat straw. The arsenic adsorption to the adsorbent loaded with different content of Fe_3O_4 is investigated. The introduction of wheat straw template can highly enhance the arsenic adsorption of Fe_3O_4. The adsorption isotherms are well fitted by Langmuir model. Based on the parameters calculated from Langmuir model, the adsorbent with higher Fe_3O_4 content has higher adsorption capacity, and the adsorption is a favorable process. The adsorption behavior is affected by pH. Moreover, this adsorbent could be regenerated and reused for at least ten cycles for arsenic adsorption. This work provided a significant avenue for effectively making use of waste biomaterials.

Acknowledgements

This work was supported by National Program on Key Basic Research Project (973 Program, No. 2011CB933700) and National Natural Science Foundation of China (No. 50773086, 50821062).

References

[1] K. Banerjee, G.L. Amy, M. Prevost, S. Nour, M. Jekel, P.M. Gallagher, C.D. Blumenschein, Kinetic and thermodynamic aspects of adsorption of arsenic onto granular ferric hydroxide (GFH), Water Res. 42 (2008) 3371–3378.
[2] V.M. Boddu, K. Abburi, J.L. Talbott, E.D. Smith, R. Haasch, Removal of arsenic(III) and arsenic(V) from aqueous medium using chitosan-coated biosorbent, Water Res. 42 (2008) 633–642.
[3] WHO, Guidelines for drinking water quality, World Health Organization, Geneva, Switzerland, 1993.
[4] M. Jang, W. Chen, F.S. Cannon, Preloading hydrous ferric oxide into granular activated carbon for arsenic removal, Environ. Sci. Technol. 42 (2008) 3369–3374.
[5] Y. Kim, C. Kim, I. Choi, S. Rengaraj, J. Yi, Arsenic removal using mesoporous alumina prepared via a templating method, Environ. Sci. Technol. 38 (2003) 924–931.
[6] J. Zhang, R. Stanforth, Slow adsorption reaction between arsenic species and goethite (α-FeOOH): diffusion or heterogeneous surface reaction control, Langmuir 21 (2005) 2895–2901.
[7] H.A. Andrianisa, A. Ito, A. Sasaki, J. Aizawa, T. Umita, Biotransformation of arsenic species by activated sludge and removal of bio-oxidised arsenate from wastewater by coagulation with ferric chloride, Water Res. 42 (2008) 4809–4817.
[8] S.A. Wasay, J. Haron, S. Tokunaga, Adsorption of fluoride, phosphate, and arsenate ions on lanthanum impregnated silica gel, Water. Environ. Res. 68 (1996) 295–300.
[9] S.F. Lim, Y.M. Zheng, S.W. Zou, J.P. Chen, Characterization of copper adsorption onto an alginate encapsulated magnetic sorbent by a combined FT-IR, XPS and mathematical modeling study, Environ. Sci. Technol. 42 (2008) 2551–2556.
[10] W. Yang, A.T. Kan, W. Chen, M.B. Tomson, pH-dependent effect of zinc on arsenic adsorption to magnetite nanoparticles, Water Res. 44 (2010) 5693–5701.
[11] X.G. Luo, L.N. Zhang, High effective adsorption of organic dyes on magnetic cellulose beads entrapping activated carbon, J. Hazard. Mater. 171 (2009) 340–347.
[12] S.F. Lim, Y.M. Zheng, J.P. Chen, Organic arsenic adsorption onto a magnetic sorbent, Langmuir 25 (2009) 4973–4978.
[13] V. Rocher, J.-M. Siaugue, V. Cabuil, A. Bee, Removal of organic dyes by magnetic alginate beads, Water Res. 42 (2008) 1290–1298.
[14] C.L. Chen, X.K. Wang, M. Nagatsu, Europium adsorption on multiwall carbon nanotube/iron oxide magnetic composite in the presence of polyacrylic acid, Environ. Sci. Technol. 43 (2009) 2362–2367.
[15] G. Huang, H. Zhang, J.X. Shi, T.A.G. Langrish, Adsorption of chromium(VI) from aqueous solutions using cross-linked magnetic chitosan beads, Ind. Eng. Chem. Res. 48 (2009) 2646–2651.
[16] C.Y. Chen, C.L. Chiang, P.C. Huang, Adsorptions of heavy metal ions by a magnetic chelating resin containing hydroxy and iminodiacetate groups, Sep. Purif. Technol. 50 (2006) 15–21.
[17] M.G. Tabka, I. Herpoel-Gimbert, F. Monod, M. Asther, J.C. Sigoillot, Enzymatic saccharification of wheat straw for bioethanol production by a combined cellulase xylanase and feruloyl esterase treatment, Enzyme Microb. Technol. 39 (2006) 897–902.
[18] R. Liu, H. Yu, Y. Huang, Structure and morphology of cellulose in wheat straw, Cellulose 12 (2005) 25–34.
[19] H. Yu, R. Liu, D. Shen, Y. Jiang, Y. Huang, Study on morphology and orientation of cellulose in the vascular bundle of wheat straw, Polymer 46 (2005) 5689–5694.
[20] R. Say, N. Yilmaz, A. Denizli, Biosorption of cadmium, lead, mercury, and arsenic ions by the fungus penicillium purpurogenum, Sep. Sci. Technol. 38 (2003) 2039–2053.
[21] C. Namasivayam, S. Senthilkumar, Removal of arsenic(V) from aqueous solution using industrial solid waste: adsorption rates and equilibrium studies, Ind. Eng. Chem. Res. 37 (1998) 4816–4822.
[22] J.F. Ferguson, J. Gavis, Review of arsenic cycle in natural waters, Water Res. 6 (1972) 1259–1274.
[23] I. Langmuir, The adsorption of gases on plane surfaces of glass, mica and platinum, J. Am. Chem. Soc. 40 (1918) 1361–1403.
[24] H. Freundlich, Concerning adsorption in solutions, Zeitschrift Fur Physikalische Chemie—Stochiometrie Und Verwandtschaftslehre 57 (1906) 385–470.
[25] M. Temkin, V. Pyzhev, Kinetics of ammonia synthesis on promoted iron catalysts, Acta Physicochim. Urss 12 (1940) 327–356.
[26] V. Chandra, J. Park, Y. Chun, J.W. Lee, I.-C. Hwang, K.S. Kim, Water-dispersible magnetite-reduced graphene oxide composites for arsenic removal, ACS Nano 4 (2010) 3979–3986.
[27] S. Yean, L. Cong, C.T. Yavuz, J.T. Mayo, W.W. Yu, A.T. Kan, V.L. Colvin, M.B. Tomson, Effect of magnetite particle size on adsorption and desorption of arsenite and arsenate, J. Mater. Res. 20 (2005) 3255–3264.
[28] J.Y. Zhang, Q. Shuai, X.G. Wang, W.Y. Du, J.H. Cheng, Removal of As(III) and As(V) from groundwater using magnetic nanonmeter-size iron oxides, China Univ Geosciences Press, Wuhan, 2009.
[29] J. Hlavay, K.r. Poly·k, Determination of surface properties of iron hydroxide-coated alumina adsorbent prepared for removal of arsenic from drinking water, J. Colloid Interface Sci. 284 (2005) 71–77.
[30] V.K. Gupta, V.K. Saini, N. Jain, Adsorption of As(III) from aqueous solutions by iron oxide-coated sand, J. Colloid Interface Sci. 288 (2005) 55–60.
[31] L. Yan, H.H. Yin, S. Zhang, F.F. Leng, W.B. Nan, H.Y. Li, Biosorption of inorganic and organic arsenic from aqueous solution by Acidithiobacillus ferrooxidans BY-3, J. Hazard. Mater. 178 (2010) 209–217.
[32] A. Maiti, S. DasGupta, J.K. Basu, S. De, Adsorption of arsenite using natural laterite as adsorbent, Sep. Purif. Technol. 55 (2007) 350–359.
[33] S. Zhang, H. Niu, Y. Cai, X. Zhao, Y. Shi, Arsenite and arsenate adsorption on coprecipitated bimetal oxide magnetic nanomaterials: $MnFe_2O_4$ and $CoFe_2O_4$, Chem. Eng. J. 158 (2010) 599–607.
[34] F. Deniz, S.D. Saygideger, Equilibrium, kinetic and thermodynamic studies of Acid Orange 52 dye biosorption by Paulownia tomentosa Steud. leaf powder as a low-cost natural biosorbent, Bioresour. Technol. 101 (2010) 5137–5143.
[35] S. Dixit, J.G. Hering, Comparison of arsenic(V) and arsenic(III) sorption onto iron oxide minerals: implications for arsenic mobility, Environ. Sci. Technol. 37 (2003) 4182–4189.
[36] N. Marmier, A. DelisÈe, F. Fromage, Surface complexation modeling of Yb(III), Ni(II), and Cs(I) sorption on magnetite, J. Colloid Interface Sci. 211 (1999) 54–60.

[37] P.L. Smedley, D.G. Kinniburgh, A review of the source, behaviour and distribution of arsenic in natural waters, Appl. Geochem. 17 (2002) 517–568.
[38] Z.X. Sun, F.W. Su, W. Forsling, P.O. Samskog, Surface characteristics of magnetite in aqueous suspension, J. Colloid Interface Sci. 197 (1998) 151–159.
[39] Y. Tian, M. Wu, R. Liu, D. Wang, X. Lin, W. Liu, L. Ma, Y. Li, Y. Huang, Modified native cellulose fibers—a novel efficient adsorbent for both fluoride and arsenic, J. Hazard. Mater. 185 (2011) 93–100.
[40] J. J^nsson, D.M. Sherman, Sorption of As(III) and As(V) to siderite, green rust (fougerite) and magnetite: implications for arsenic release in anoxic groundwaters, Chem. Geol. 255 (2008) 173–181.